

AD-A173 540

CHARACTERISTICS OF PT THIN FILMS ON TiO₂(110) TEXAS
UNIV AT AUSTIN DEPT OF CHEMISTRY Y SUN ET AL.

1/1

UNCLASSIFIED

01 SEP 86 TR-49 N00014-83-X-0382

F/G 7/4

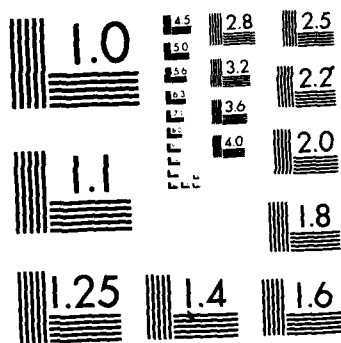
NL

END

DATE

FILED

12-86



MICROCOPY RESOLUTION TEST CHART
NATIONAL BUREAU OF STANDARDS-1963-A

AD-A173 540

12

OFFICE OF NAVAL RESEARCH

Contract No. N00014-83-K-0582

Task No. NR 056-578

TECHNICAL REPORT NO. 49

CHARACTERISTICS OF Pt THIN FILMS ON $\text{TiO}_2(110)$

Prepared for publication

in

The Journal of Physical Chemistry

Y.-M. Sun, D. N. Belton and J. M. White

Department of Chemistry

The University of Texas at Austin

Austin, Texas 78712

651 10 01 98

DTIC FILE COPY

Reproduction in whole or in part is permitted for any purpose of the United States Government.

This document has been approved for public release and sale; its distribution is unlimited.

DTIC
ELECTE
OCT 24 1986
S B D

SECURITY CLASSIFICATION OF THIS PAGE (When Data Entered)

REPORT DOCUMENTATION PAGE		READ INSTRUCTIONS BEFORE COMPLETING FORM
1. REPORT NUMBER	2. GOVT ACCESSION NO.	3. RECIPIENT'S CATALOG NUMBER
4. TITLE (and Subtitle) Characteristics of Pt Thin Films on TiO_2 (110)		5. TYPE OF REPORT & PERIOD COVERED Technical Report #49 January 1 - December 31, 1985
7. AUTHOR(s) Y.-M. Sun, D. N. Belton and J. M. White		6. PERFORMING ORG. REPORT NUMBER
8. PERFORMING ORGANIZATION NAME AND ADDRESS J. M. White, Department of Chemistry University of Texas Austin, TX 78712		9. CONTRACT OR GRANT NUMBER(s) N00014-83-K-0582
11. CONTROLLING OFFICE NAME AND ADDRESS Department of the Navy Office of Naval Research Arlington, VA 22217		10. PROGRAM ELEMENT PROJECT TASK AREA & WORK UNIT NUMBERS Project No. NR-056-578
14. MONITORING AGENCY NAME & ADDRESS (if different from Controlling Office)		12. REPORT DATE 9-1-86
		13. NUMBER OF PAGES 14
		15. SECURITY CLASS (of this report)
		15a. DECLASSIFICATION DOWNGRADING SCHEDULE
16. DISTRIBUTION STATEMENT (of this Report) Approved for public release; distribution unlimited.		
17. DISTRIBUTION STATEMENT (of the abstract entered in Block 20, if different from Report)		
18. SUPPLEMENTARY NOTES		
19. KEY WORDS (Continue on reverse side if necessary and identify by block number)		
20. ABSTRACT (Continue on reverse side if necessary and identify by block number) Thin films of Pt on oxidized and reduced forms of TiO_2 have been studied under UHV conditions. XPS and depth profile data support migration of reduced Ti oxide to the Pt surface (encapsulation) when a reduced sample is annealed above 400°C. On the fully oxidized sample, annealing caused delinking of the Pt layer but no encapsulation. XPS characterization of the encapsulating species indicates that Ti is present primarily as Ti^{2+} .		

DD FORM 1 JAN 73 1473

EDITION OF 1 NOV 65 IS OBSOLETE
S/N 0102-014-6601

SECURITY CLASSIFICATION OF THIS PAGE (When Data Entered)

JP8507 12.

J. Phys. Chem.
Submitted

(201)

Characteristics of Pt Thin Films on $\text{TiO}_2(110)$ (a)

by

Y.-M. Sun(b), D. N. Belton(c) and J. M. White

University of Texas
Department of Chemistry
Austin, TX 78712

(a) Supported in part by the Office of Naval Research.

(b) Present address: Tsinghua University
Beijing, China

(c) Present address: General Motors Research Laboratories
Warren, MI 48090

ABSTRACT

Thin films of Pt on oxidized and reduced forms of TiO_2 have been studied under UHV conditions. XPS and depth profile data support migration of reduced Ti oxide to the Pt surface (encapsulation) when a reduced sample is annealed above 400 °C. On the fully oxidized sample, annealing caused islanding of the Pt layer but no encapsulation. XPS characterization of the encapsulating species indicates that Ti is present primarily as Ti^{2+} .

Acco	
Dist	
Avail	
Dist	Sp
A-1	



1. Introduction

Over the last 6 years there has been considerable interest in the topic of strong metal support interactions, SMSI.[1,2] The reductions in hydrogen and CO chemisorption, concurrent with increases in specific activity for the methanation reaction [3,4], sparked hope of entirely new possibilities for catalyst modification and control. These observations and their discussion are related to earlier work.[5] Four mechanisms -- "pill-box" morphology, charge transfer, local intermetallic bonding, and encapsulation -- have been proposed to explain the observed phenomena. Recently more and more evidence, primarily from model catalyst studies [6-10], has appeared which supports encapsulation as a major effect in these SMSI systems. There is, however, also good evidence for electronic (bonding) effects.[6,11] Structural characterization of the encapsulating species, the effect of encapsulation on reactivities, and the alteration of the electronic structure of the metal by the encapsulating species are still incompletely understood SMSI issues.

In earlier work we showed that encapsulation of Pt or Rh layers occurs on oxidized Ti(0001)[6]. Similar results were also obtained by Chung et. al. [10] for Ni on oxidized Ti foil. While the results were convincing for these models, it is debatable whether the 60-100 Å TiO_2 overlayer present on bulk Ti is representative of bulk rutile or anatase. Structural differences and the semi-infinite amount of zero-valent Ti, not present in bulk TiO_2 , could lead to encapsulation in these models. The work of Sadeghi and Henrich [9] answers this question for Rh by showing that encapsulation does occur. They studied Rh on $\text{TiO}_2(110)$ using AES, XPS and TPD with depth profiling. For 1.5 to 4 equivalent monolayers of Rh on fully oxidized TiO_2 ,

(no Ti^{2+} in XPS), heating either in 10^{-7} Torr H_2 or in UHV for 30 min at 673K lead to encapsulation of the Rh by a reduced form of titania. As compared to a sample that was not heated, the $Ti(2p)$ XPS region had more intensity toward lower binding energies, the AES peak-to-peak Ti/O ratio was higher, the ability to chemisorb CO was diminished and the depth profile had a local maximum in the Rh AES signal. After some sputtering, the heated sample regained its ability to chemisorb CO. There was evidence for some islanding during heating, but no evidence for migration of Rh into the TiO_2 .

While the evidence is now clear that encapsulation is a major, but not the only factor, affecting the SMSI character of these Group VIII metal-titania systems, little attention has been given to variations with the metal. Since Pt oxides are less stable than Rh oxides and since the ionization potential of Pt (9 eV) is significantly greater than that of Rh (7.35 eV), we thought intuitively that detectable differences might occur in the two systems. To explore this possibility and to further characterize encapsulating species, we have examined Pt on single crystal $TiO_2(110)$.

II. Experimental

The experiments were performed in a VG ESCALAB spectrometer equipped with a dual anode x-ray source for XPS, electron gun for AES, and an ion gun for sputtering. Metal depositions were done in a UHV preparation chamber attached to the analysis chamber and used a resistively heated metal evaporation source consisting of a tungsten filament wrapped with Pt wire. The substrate remained below 50°C during Pt deposition. The thickness of the metal layers was estimated from attenuation of the $Ti(2p)$ XPS peak assuming a mean free path of about 10 Å.

A sample holder and heating device were designed to allow heating of

the sample to 770 °C in the preparation chamber. The TiO₂ single crystal was clamped to a Ta foil backing plate with a Ta wire. The sample was indirectly heated by conduction from the resistively heated Ta foil. Temperatures were determined with a chromel-alumel thermocouple attached to the Ta foil.

The single crystal TiO₂ sample was cleaned by successive ion bombardment and annealing cycles. After cleaning, no impurities were detected by XPS. A fully oxidized surface was prepared by heating the sample to 500°C in 10⁻⁶ Torr of O₂. A partially reduced surface was prepared by Ar⁺ sputtering.

III. Results

III.1. Pt on oxidized TiO₂(110)

Figure 1a shows the XPS Ti(2p) region of the fully oxidized TiO₂ single crystal before the Pt deposition. The Ti(2p_{3/2,1/2}) peak positions of 459.2 and 465.0 are consistent with reported literature values and indicate that sample charging is not occurring.[12] After deposition of Pt (at 25°C), the Ti(2p) peak intensity (Fig.1b) is reduced to about 10% of its initial value, indicating that the Pt layer is about 20Å thick. No information about the growth mode of Pt can be obtained from this data; however, we expect that it is similar to Pt growth on oxidized Ti(0001) where layered growth is favored over three dimensional islanding.[5]

The Pt(4f) XPS for the deposited layer is shown in Fig. 2a. The Pt(4f_{7/2}) binding energy is 71.1 eV which is in excellent agreement with published results for Pt foils and single crystals.[13] The sample was repeatedly transferred to the preparation chamber where it was annealed to successively higher temperatures with XPS characterization at each stage.

6

Figures 2b-d, and 3a-c show the Pt(4f) and Ti(2p) regions, respectively, for annealing to 300, 400, and 500°C. As the annealing temperature increases: (1) the Pt peak areas gradually decrease (annealing to 500°C reduced the Pt signal by 25%), (2) the Pt(4f) and Ti(2p) peak positions remain constant, and (3) the Ti(2p) signals increase (the Ti(2p) peak area increases by a factor of 3.5 after heating to 500 °C).

After annealing to 500°C, the sample was depth profiled with Ar⁺ sputtering (5 KeV, 5 µA) using 15 second intervals. With sputtering, the Ti(2p) region (Fig.4) underwent two changes (summarized in Fig. 7). First, the total Ti(2p) intensity increased monotonically with increased Ar⁺ dose due to removal of surface Pt. Second, the Ti(2p) intensity increased at low binding energies, particularly after sputtering for 30 seconds or longer. The peak width increased due to preferential sputtering of oxygen, introducing Ti species with valencies less than +4. With sputtering, the Pt peak areas decreased monotonically but there was no measureable shift of binding energy. Because the Ti(2p) FWHM does not change until after 30 seconds of sputtering, the data suggests that very little TiO₂ (rather, mainly Pt) was exposed at the beginning of the depth profile.

The XPS data of Figs. 2-4 suggest the following: (1) upon annealing, Pt overlayers form islands, (2) little or no TiO₂ is exposed when the islands are formed, (3) the underlying TiO₂ is unchanged by the annealing procedure and remains fully oxidized, (4) when TiO₂ is sputtered oxygen is preferentially removed forming reduced Ti centers.

In a separate experiment one monolayer of Pt was deposited on a fully oxidized substrate. Just as for the thicker 20Å Pt case, upon sputtering the Pt(4f) intensity decreased monotonically and the binding energy remained constant, suggesting that significant interdiffusion of Pt into TiO₂ did not

7

occur. Significantly, TiO_2 deposited on bulk Pt does diffuse at temperatures above 450°C [14-15].

III.2. Pt on Reduced $\text{TiO}_2(110)$

In order to better represent processes that occur in a strongly reducing environment, a partially reduced oxide surface was prepared by removing some oxygen by Ar^+ sputtering. Figure 5a shows the results of sputtering the $\text{TiO}_2(110)$ surface for 1 hour with 5 KeV Ar^+ ions. The broad unresolved nature of the spectrum indicates that reduced Ti species are present. The low binding energy onset is below 455 eV and, with evidence presented below, the lowest valence of significance is Ti^{2+} . Figure 5b shows the $\text{Ti}(2p)$ region after the deposition of about 25Å of Pt. The $\text{Ti}(2p)$ peaks were strongly attenuated and, due to the broadness of the peaks on this reduced surface, are very hard to discriminate from the background.

After annealing this sample at 500°C , the Ti peak area increased by about a factor of 2. In addition, the peak shape becomes slightly more distinct, centered at about 455 eV and is best described as a mixture of Ti^{2+} and Ti^{3+} (see Fig. 6). The Pt peak area decreased 20% after annealing at 500°C , but there were no observable changes in line shape or position. The $\text{O}(1s)/\text{Ti}(2p)$ peak area ratio (including relative sensitivities) indicates $0.9 \leq \text{O}/\text{Ti} \leq 1.1$.

After annealing at 500°C , the sample was depth profiled. Figure 6 shows the $\text{Ti}(2p)$ region before (Fig. 6a) and at several times during the depth profile. Before sputtering, the FWHM and position of the $\text{Ti}(2p)$ peak reflects the presence of more than one oxidation state. The intensity of the peak at 454.4 eV and its continued presence even after 55 sec of

sputtering (lower binding energy shoulder in Fig. 6d) indicate that the dominant oxidation state is Ti^{4+} . [12] Upon sputtering, the $Ti(2p)$ signal broadens and shifts to higher binding energies, indicating that more fully oxidized Ti species are appearing. It is significant that there is a rather strong shift to higher binding energy between 25 and 55s sputtering time (Figs. 6(c) and 6(d)). Because the shift is toward more oxidized Ti species, the sputtering process itself is not responsible since sputtering reduces titania surfaces. That the binding energy shift is rather sudden is consistent with a model in which some of the reduced titania covers (encapsulates) the Pt which itself tends to island. This is discussed in more detail below. Deeper into the substrate (Fig. 6e), Ti^{4+} was detected, as expected, but a shoulder toward lower binding energy was evident indicating the presence of some partially reduced species.

Figure 7 summarizes the depth profile data for Ti (top panel) and Pt (bottom panel) from the two substrates. For the oxidized substrate (triangles), the $Ti(2p)$ intensity (top panel) increases monotonically as a function of time. The reduced sample (circles) differs in that it shows a slight decrease in Ti peak area between zero and 20 seconds sputtering time. The Pt data (bottom panel) drops monotonically for the oxidized but has a local maximum at 20s for the reduced sample. The $Ti(2p_{3/2})$ peak positions for the two different samples are compared in the bottom panel of Fig. 7). The oxidized sample (open triangles) shows no shift in peak position (the spectrum does broaden) as a function of sputtering time indicating the dominance of one type of Ti (from the TiO_2 substrate). The reduced sample (open circles) shows a strong shift to higher binding energy as the substrate begins to contribute to the spectrum. For the oxidized sample (Fig. 7), the initial region of constant FWHM (upper

panel of Fig. 7) of the Ti(2p) signal is followed by a linearly increasing region corresponding to the sputtering of bare patches of TiO_2 . This is evidence that no TiO_x species cover the Pt after annealing the fully oxidized sample. On the reduced sample (open circles) there is an initial region of constant FWHM followed (after 30 s) by a sharp increase and a slower decline to a value close to that reached for the fully oxidized sample. Note that 30 s is near the point where the total Ti intensity also increases. We interpret these data for the reduced case in terms of a surface highly enriched in reduced oxides. Since sputtering can not further reduce the surface, the Ti(2p) linewidth does not change very much initially. After 30 seconds the linewidth and the increasing Ti(2p) binding energies indicate that more highly oxidized species (from the original substrate) lie within the XPS sampling volume. The combined signals from the both the reduced and oxidized species give a very broad peak. Beyond 50 s sputtering, surface TiO_x (reduced sample) is completely removed and the FWHM decreases.

These data demonstrate that the thermal behavior of Pt on TiO_2 varies depending on the initial condition of the substrate. For the initially reduced $\text{TiO}_2(110)$ surface, the data are consistent with the encapsulation of the Pt by TiO_x ($0.9 \leq x \leq 1.1$), but unlike the case for Rh [9], there is no evidence for encapsulation when the substrate is fully oxidized prior to Pt deposition.

IV. DISCUSSION

In previous work we reported that Pt or Rh supported on oxidized

Ti(0001) became encapsulated by TiO_x ($x > 1$) when the sample was annealed above 350°C [6]. The work presented here confirms that the encapsulation observed in that study was not simply due to the thin (60 Å) TiO_2 layer present on the bulk Ti sample. The depth profile data (Fig. 7) shows that encapsulation occurs for the prerduced Pt/ TiO_2 sample but not for the fully oxidized sample. The initial decrease in the Ti intensities and the increase in Pt intensities can be explained only by a surface rich in Ti as reported earlier for Rh on $\text{TiO}_2(110)$ [9].

Pt (this work) and Rh (ref. 9) differ in that, for a fully oxidized substrate, there is evidence for encapsulation on the latter but not the former. That there is negligible encapsulation for Pt on oxidized TiO_2 is evident in Fig. 7 where the monotonic increase and decrease in the Ti and Pt signals, respectively, are not compatible with encapsulation. Changes in the Pt and Ti XPS intensities were observed and can be understood in terms of islanding of Pt and/or interdiffusion of the Pt and TiO_2 . Although interdiffusion can not be completely eliminated, particularly for the 20 Å Pt overlayer, the data (thin and thick initial Pt layers) are best described in terms of islanding where no large bare patches of TiO_2 are exposed during annealing to 500°C . If bare patches of clean TiO_2 were produced then the Ti(2p) FWHM would increase at the start of the depth profile, as is always seen when sputtering a clean TiO_2 surface.

Besides demonstrating that encapsulation of Pt occurs on bulk TiO_2 samples if reduced surface Ti is present, the experiments provide XPS characterization of the encapsulating species. Comparison of the XPS data shown in Fig. 6a with other Ti oxides shows the Ti is best described as Ti^{4+} with considerable Ti^{3+} [13]. The data of Figs. 6 and 7 show that Fig. 6a is not dominated by substrate signals (i.e. this spectrum detects mainly

a signal due to encapsulation). As Pt was removed from the sample by sputtering, the substrate signal contributed more to the total Ti intensity and Fig. 6e shows that the underlying substrate is more oxidized than the encapsulating layer. There are at least two reasons why the substrate appears oxidized after annealing to 500°C when it is reduced prior to Pt deposition. First, the defects introduced into TiO₂ by sputtering tend to be removed by heating, even in the absence of Pt. Second, a significant fraction of the reduced Ti migrates to the surface of the Pt overlayer. According to our view, encapsulation is aided by a reduced source of Ti. This is consistent with our earlier work [6] where one role of the Ti(0001) underlying a thin film of TiO₂ is to promote the formation of reduced Ti for encapsulation.

It is interesting to compare the results obtained here with similar experiments conducted on powder systems. Work by Chen and White [16] showed suppression of CO and H₂ uptake for Pt supported on prerduced TiO₂ powders. In that study annealing in vacuum (as opposed to reduction in H₂) resulted in the loss of CO and H₂ uptake. The encapsulation found here will account for those observations. Dwyer *et al.* [17] showed by ion scattering and thermal desorption that simple site blocking by submonolayer coverages of TiO₂ on bulk Pt could account for most of the loss of CO chemisorption in SMSI systems. However, in earlier thin film work [6], there is evidence for the contribution of a local electronic effect.

We now turn to a discussion of possible encapsulation processes. In a series of papers, Spencer [18-21] has discussed segregation and diffusion in Pt/TiO₂ on the basis of a broken bond model. There are two factors which control the thermodynamics of segregation: (1) a strain energy related to the mismatch of the sizes of the atoms (big impurity atoms will segregate if

they are in a small atom lattice) and (2) a surface free energy due to the bonding between atoms (an impurity atom will segregate if it is more weakly bound by the host lattice than a host atom itself). For Ti in Pt, Ti is small so the strain component does not favor or disfavor segregation. The free energy of a Pt-Ti bond (22.6 kcal/mol) is larger than for a Pt-Pt bond (17.7 kcal/mol) so the Ti will not occupy the surface (i. e. the surface will be Pt-rich). In the presence of oxygen, TiO_x will segregate to the surface (or migrate there across the Pt) because the Ti-O bond is so strong (70.0 kcal/mol). This will become even more dominant if the Pt-O-Ti bonding is especially strong. Spencer also discusses the mechanism of the covering of Pt by TiO_x ; he favors the transport of this species across the Pt surface (assisted by the mobility of the Pt) after its formation at Pt- TiO_2 boundaries. According to this mechanism, segregation is thermodynamically favored, even at temperatures below those characteristic of SMSI ($\leq 500^\circ C$), but kinetically it is strongly inhibited.

One model, consistent with our observations, is based on Spencer's [18] suggestion that TiO_x forms at Pt/ TiO_2 interfaces and is transported along grain boundaries to the surface and then across the Pt surfaces. In earlier work using SIMS, we found that heating in UHV to encapsulate metals on $Ti^{18}O_2$ layers always leads to the formation of ^{18}O -labelled TiO_x ($1.0 \leq x \leq 1.2$). Thus, the oxygen involved in the encapsulating surface layer also migrates from the Pt- TiO_2 interface and is not derived from background gases such as water. Based on diffusion rates of oxygen atoms in bulk Pt at $500^\circ C$ [22] ($E_d > 53$ kcal/mole and $D_0 = 10$ cm²/sec, $D = 10^{-11}$ cm² sec⁻¹), the mean distance travelled by an oxygen atom in 200 sec is only 0.06Å. This is insufficient to account for the appearance of saturation amounts of encapsulating TiO_x in 200 sec. [6] Thus, it is unlikely that either O or TiO

migrates through the Pt bulk. To account for the observed appearance of TiO_x in ≈ 200 sec through a 30A Pt film requires an effective diffusion rate constant that is four or five orders of magnitude higher (data for overlayers between 10 and 30A thick are consistent with a diffusion coefficient between 10^{-17} and $10^{-16} \text{ cm}^2 \text{ sec}^{-1}$). This is consistent with diffusion along grain boundaries [22], and we suggest this as the most likely mechanism.

The fact that there is no evidence for encapsulation, unless the $\text{TiO}_2(110)$ surface is sputtered before adding the Pt, points to the importance of rather strong chemical interactions at the interfaces between Pt and reduced titania. In the absence of significant concentrations of these reduced centers, the Pt-titania interactions are apparently much weaker and, more importantly, the rate of their formation is slow compared to the mobility of Pt which leads to three dimensional islanding. That these rates are competitive is indicated by the fact that the same thermal treatment that leads to only islanding for the fully oxidized surface leads to encapsulation when the surface is prereduced. In fact, our results are consistent with a model in which both encapsulation and islanding contribute measurably for the prereduced sample.

Spencer [21] points out that Pt atoms should be mobile at 450°C and higher. The observed three dimensional islanding on fully oxidized bulk $\text{TiO}_2(110)$ is consistent with this notion. This mobility may also play a role in the kinetics of the encapsulation; Pt-O-Ti moieties formed at the interface will move away from the interface and across the surface "carried" by the motion of the surrounding Pt atoms.

Turning to a comparison of Pt and Rh, Ko and Gorte [14] have studied thin layers of TiO_2 deposited on Pt and Rh foils. They observe interesting

differences in the two metals. Upon heating a monolayer of titania to 1000° C, it was incorporated into the bulk of the Pt film and reseggregated to the surface on cooling. By contrast, on Rh the oxide remained on the surface to 1100° C (the highest temperature studied). When multilayers of titania on Rh were heated to 1100° C, the remaining surface oxide layer could be sputtered off at room temperature. When the sample was reheated, TiO segregated to the surface indicating that incorporation of TiO into the bulk of Rh does occur. Apparently the Rh-O-Ti interaction is stronger than Pt-O-Ti. This difference is consistent with negligible encapsulation of Pt (our observation) on fully oxidized TiO₂(110), whereas there is significant encapsulation of Rh [9].

The encapsulation of Rh and Pt thin films on oxidized Ti(0001) have the same time characteristics to within our experimental reproducibility which is about $\pm 50^\circ \text{C}$ for the onset temperature and $\pm 100 \text{ sec}$ for the time required to reach a constant SIMS intensity after reaching 500° C [6]. Were encapsulation closely related to the ease with which Pt and Rh are oxidized, some distinction might appear because the ionization potentials of Pt and Rh are 9.0 and 7.46 eV, respectively [23]. It is also well known that oxides of Rh are more stable than those of Pt. Thus, on the thin film models [9], factors other than the differences in the electronic properties of Pt and Rh control the mechanism of encapsulation, whereas on single crystal TiO₂(110) these differences are important. Defect formation on the latter may be important for the kinetics whereas for the thin films the migration through the grain boundaries likely controls the kinetics.

V. SUMMARY

The results of the experiments presented here can be summarized as

follows:

- (1) On a fully oxidized $\text{TiO}_2(110)$ substrate Pt overlayers island upon annealing between 300-500°C without exposure of large bare TiO_2 patches.
- (2) On reduced $\text{TiO}_2(110)$, oxides present at the Pt- TiO_2 interface migrate through grain boundaries and over the Pt surface when the sample is annealed above 400°C.
- (3) Reduced Ti oxides at the Pt- TiO_2 interface tend to stabilize Pt overlayers and restrict islanding.
- (4) XPS data indicate that the reduced TiO_x species that encapsulates the Pt surface contains mostly Ti^{2+} and that $x \approx 1$.

References

1. "Metal Support and Metal Additive Effects in Catalysis", B. Imelik et. al., Ed., Amsterdam, and references therein.
2. G.C. Bond and R. Burch, Catalysis, 6, 27(1983), and references therein.
3. S.J. Tauster, S.C. Fung, and R.L. Garten, J. Amer. Chem. Soc., 100,170(1978).
4. S.J. Tauster and S.C. Fung, J. Catal., 55, 29(1978).
5. See F. Solymosi, Catal. Rev. 1,233(1967) for example.
6. D.N. Belton, Y.-M. Sun, and J. M. White, J. Phys. Chem., 88, 5172(1984).
7. R.T.K. Baker, E.B. Prestridge, and G.B. McVicker, J. Catal., 88, 422(1984).
8. A.J. Simoens, R.T.K. Baker, D.J. Dwyer, C.R.F. Lund, and R.J. Madon, J. Catal., 86,359(1984).
9. H.R. Sadeghi and V.E. Henrich, J. Catal., 87,279(1984).
10. Y.-W. Chung, G. Xiong, and C.-C. Kao, J. Catal., 85, 237(1984).
11. H.-C. Loye and A. M. Stacy, J. Am. Chem. Soc. 107(1985)4657.
- 12 a. L. Ramquist, K. Hamrin, G. Johansson, A. Fahlmann and C. Nordling, J. Phys. Chem. Solids, 31, 2669 (1970).
- 12 b. M. Murata, K. Wakino and S. Ikeda, J. Electron Spectry., 6, 459 (1975).
13. C. D. Wagner, W. M. Riggs, L. E. Davis, J. F. Moulder and G. E. Mullenberg. Handbook of X-ray Photoelectron Spectroscopy (Physical Electronics Ind. Inc., 1979) p. 68.
14. C. S. Ko and H. J. Corte, J. Catalysis, 90, 59 (1984).

15. C. M. Greenlief, J. M. White, C. S. Ko and R. J. Corte, J. Phys. Chem. 89(1985)5025.
16. B.-H. Chen and J. M. White, J. Phys. Chem., 86, 3534(1982).
17. D. J. Dwyer, S. D. Cameron and J. L. Gland, J. Vac. Sci. Technol. A3, 1569 (1985).
18. M. S. Spencer, Abstracts, Division of Petroleum Chemistry, American Chemical Society, 30,157(1985).
19. M. S. Spencer, Surface Sci. 145,145(1984).
20. M. S. Spencer, Surface Sci. 145,153(1984).
21. M. S. Spencer, J. Catalysis, 93,216(1985).
22. L. R. Velho and R. W. Bartlett, Metallurgical Trans. 3,65(1972).
23. CRC Handbook of Chemistry and Physics, 52nd Edition, Robert E. Weast, Ed., Chemical Rubber Co., Cleveland (1971).

FIGURE CAPTIONS

Figure 1a: Ti(2p) XPS of the clean TiO₂(110) single crystal prior to metal deposition. 1b: Ti(2p) region of the sample in 1a after deposition of 20 Å Pt.

Figure 2: Pt(4f) XPS of 20 Å Pt on TiO₂ after annealing for 10 minutes at the temperatures indicated at the right of the spectrum.

Figure 3: Ti(2p) XPS of 20 Å Pt on fully oxidized TiO₂ of fig.1a after annealing for 10 minute at the temperature indicated at the right of the spectrum.

Figure 4: Ti(2p) XPS data of the obtained during the depth profile of the annealed Pt/TiO₂. The substrate was the fully oxidized TiO₂. The length of sputtering is, (a) through (e), 0, 15, 30, 60, and 150 s.

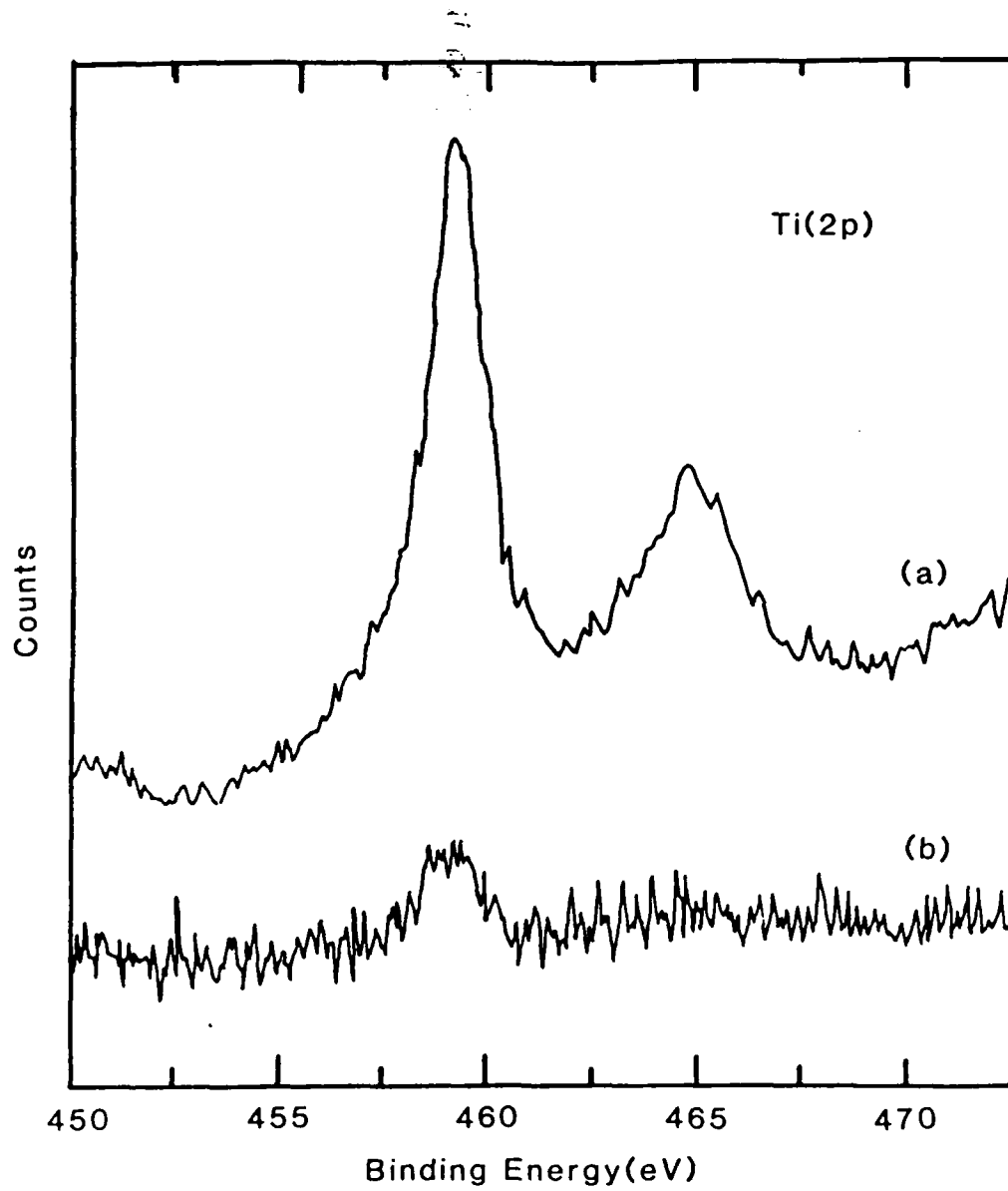
Figure 5a: Ti(2p) XPS data of the reduced TiO₂(110) sample prior to metal deposition. 5b: Sample in 5a after deposition of 25 Å Pt.

Figure 6: Ti(2p) data obtained at various points during the depth profile of the annealed Pt/ reduced TiO₂ sample. Curve (a) is after annealing for 10 min at 500°C and no sputtering. Curves (b)-(e) are for 5, 25, 55 and 115 s sputtering.

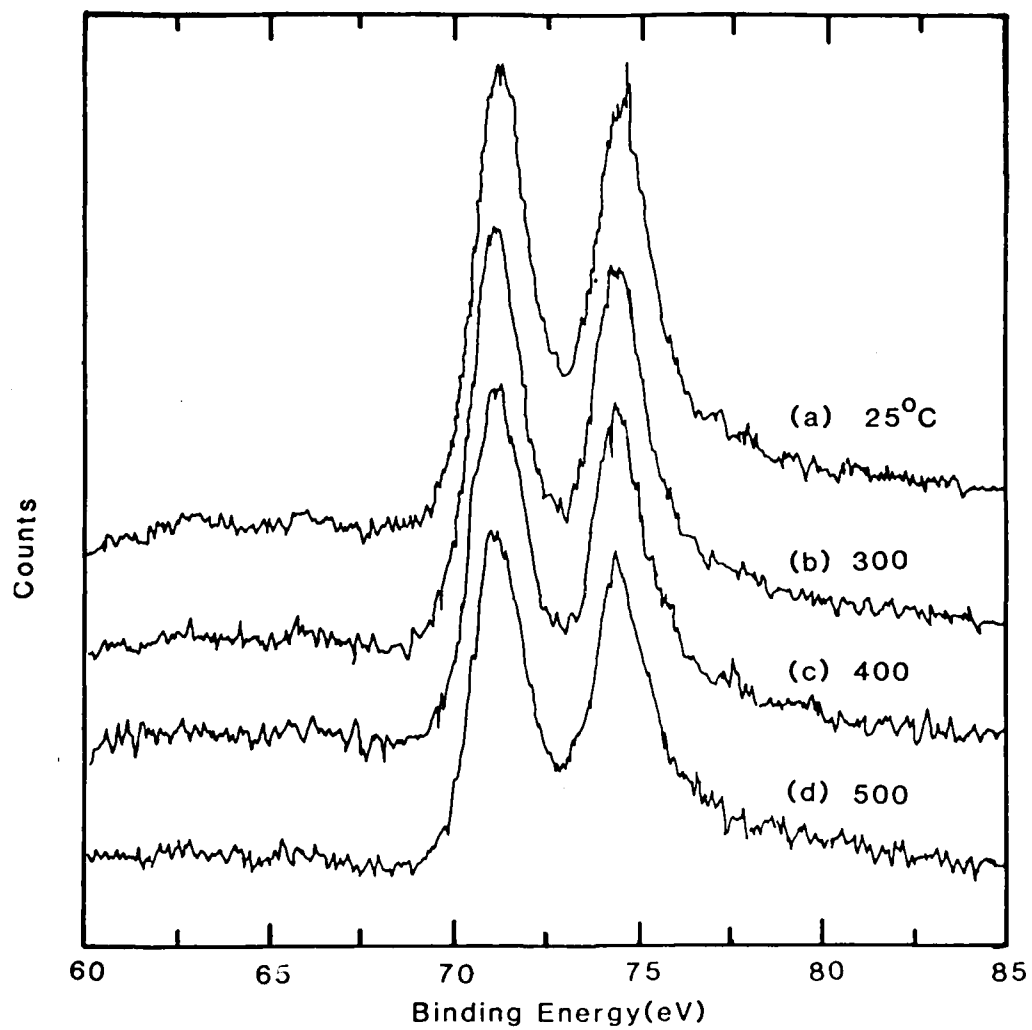
Figure 7: Relative integrated peak areas for Ti(2p) (top) and Pt(4f) (bottom) as a function of sputtering time. Also shown are FWHM data for

14

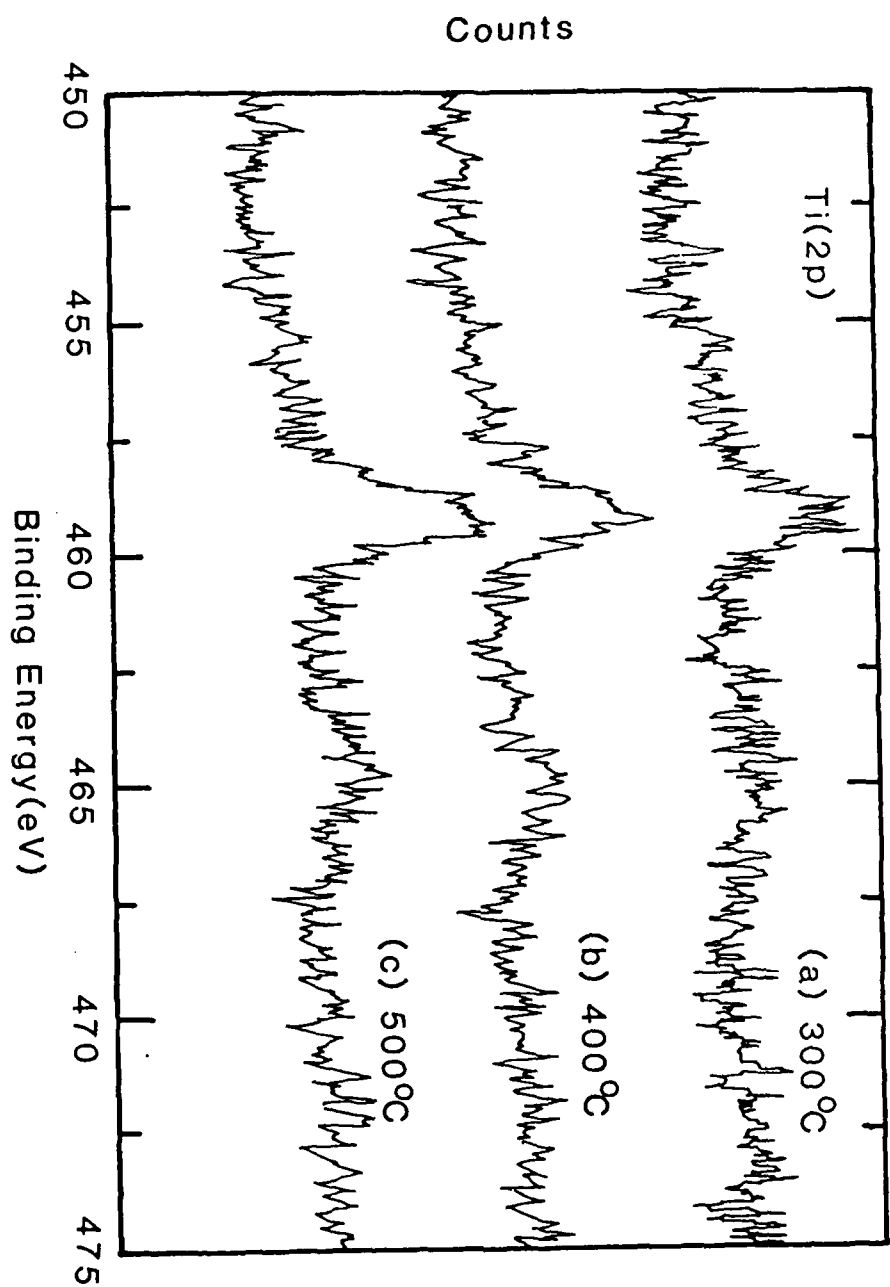
Ti(2p_{3/2}) (top) and Ti(2p_{3/2}) BE (bottom). Triangles are data for oxidized TiO₂(110) and circles for the prereduced TiO₂(110).

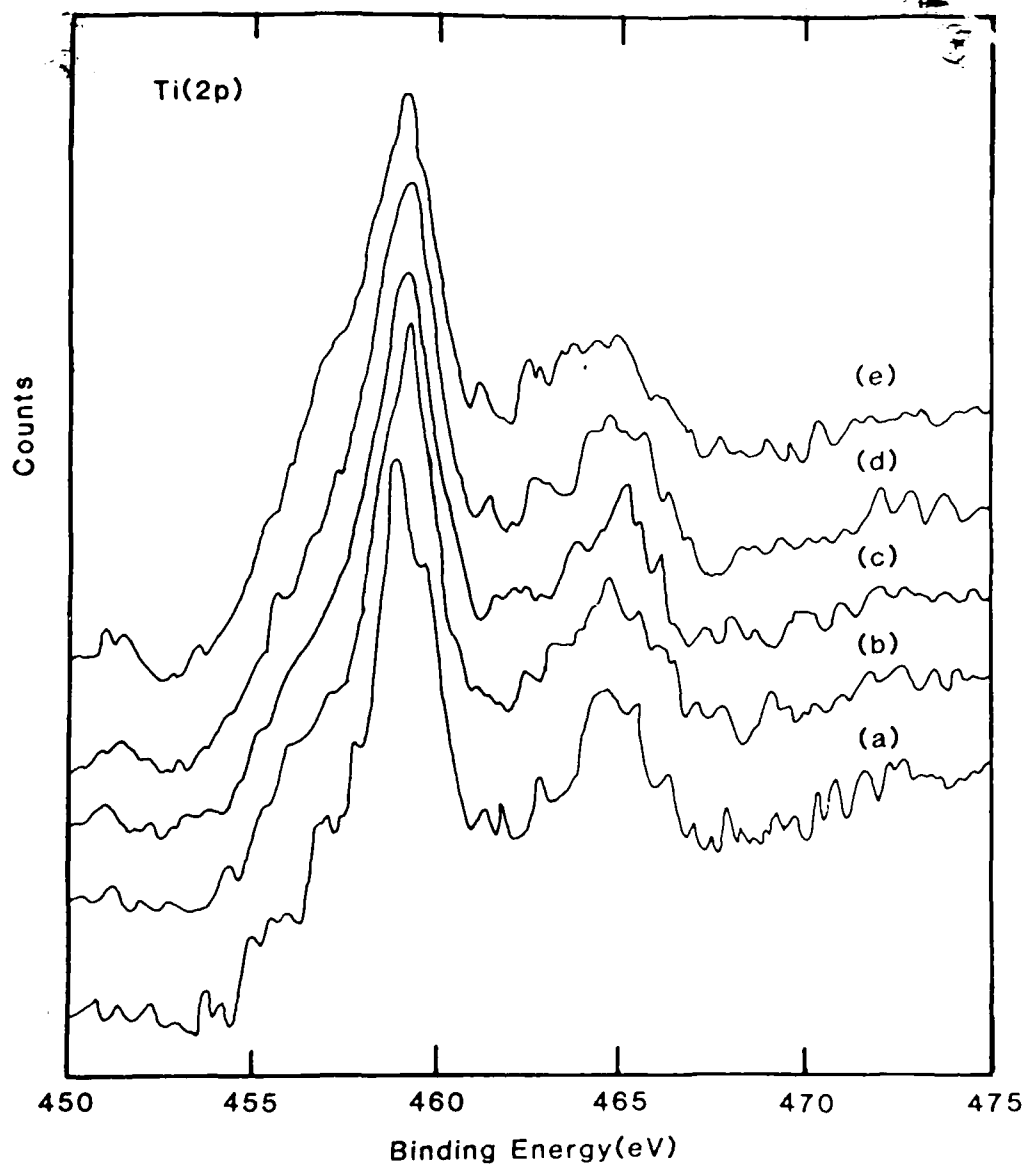


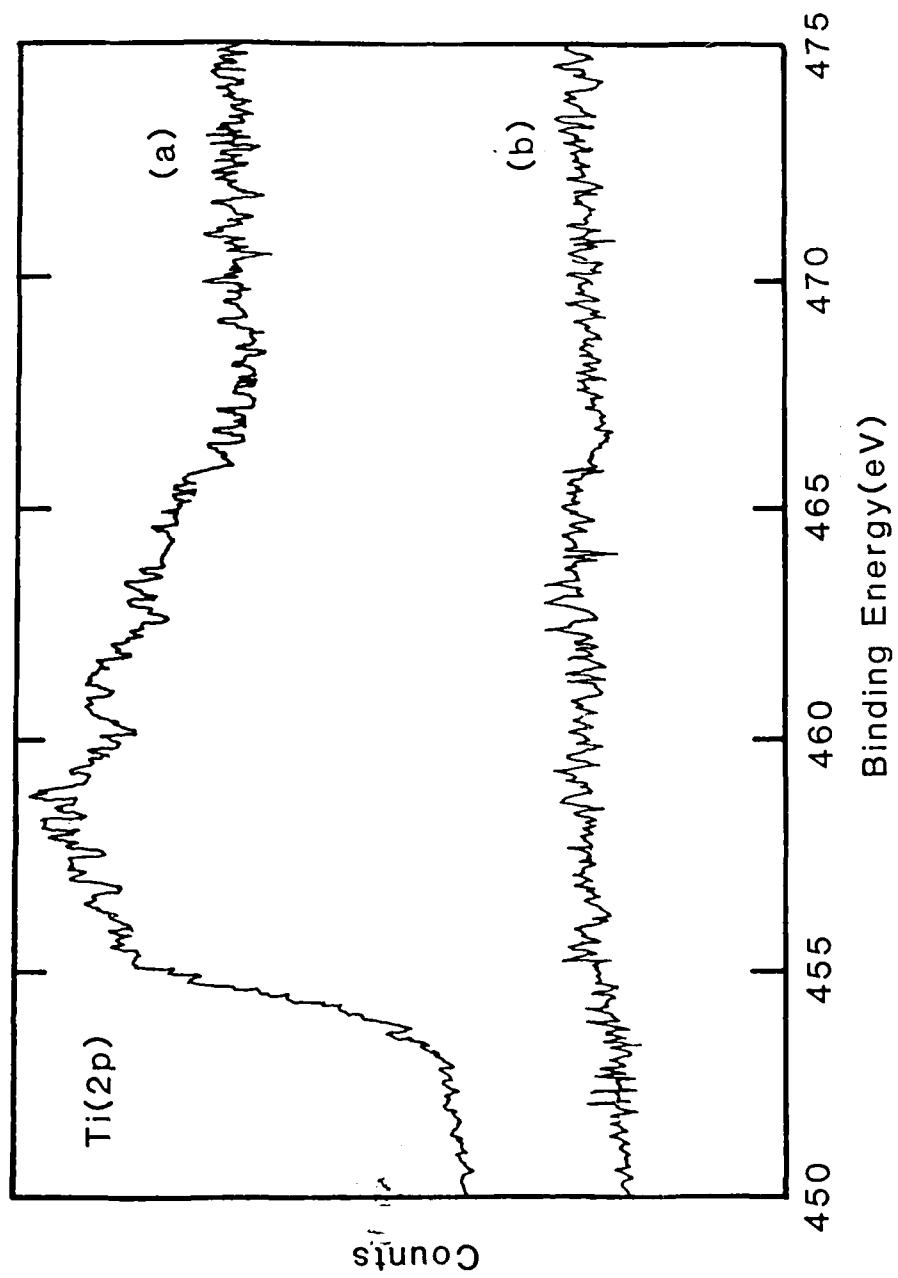
JP850561L
Fig. 1

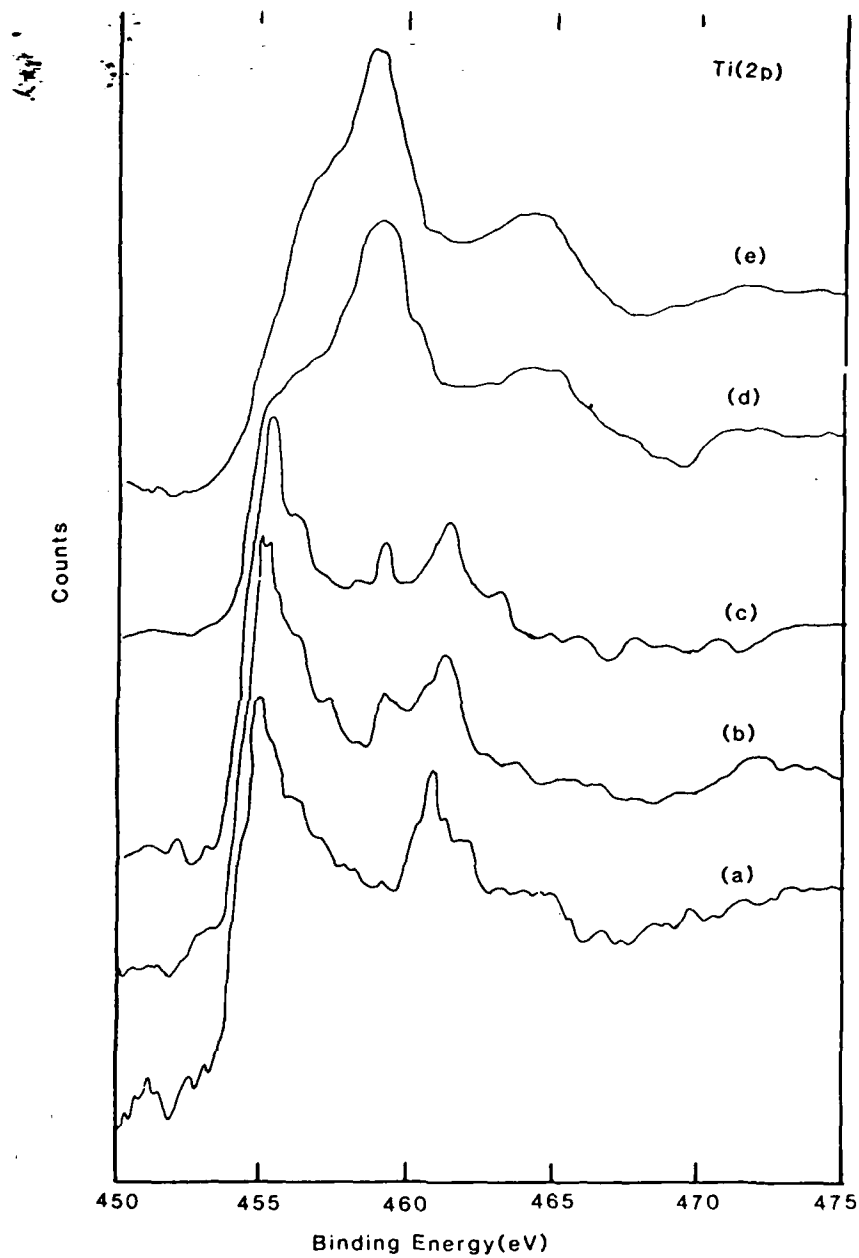


JP8505611.
Fig. 2

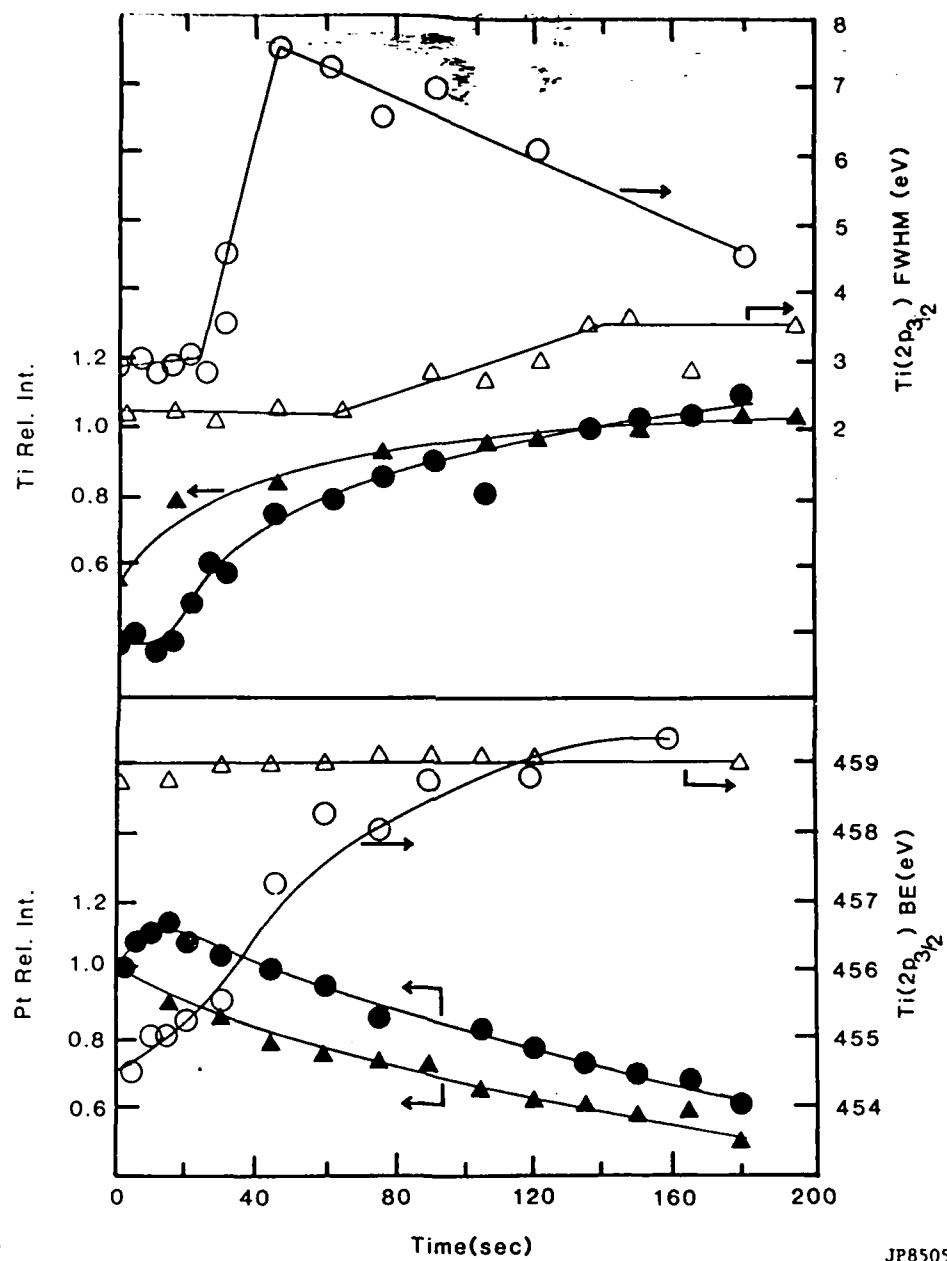








JP850561L
Fig. 6



JP850561L
Fig. 7 -

DATE
FILMED
2-8